Stochastic multiresonance in the coupled relaxation oscillators

E. I. Volkov[a)]
Department Theoretical Physics, Lebedev Physical Institute, Leninskii 53, Russia

E. Ullner[b)] and J. Kurths[c)]
Institut für Physik, Potsdam Universität, Am Neuen Palais 10, D-14469 Potsdam, Germany

(Received 15 December 2004; accepted 9 March 2005; published online 27 April 2005)

We study the noise-dependent dynamics in a chain of four very stiff excitable oscillators of the FitzHugh–Nagumo type locally coupled by inhibitor diffusion. We could demonstrate frequency- and noise-selective signal acceptance which is based on several noise-supported stochastic attractors that arise owing to slow variable diffusion between identical excitable elements. The attractors have different average periods distinct from that of an isolated oscillator and various phase relations between the elements. We explain the correspondence between the noise-supported stochastic attractors and the observed resonance peaks in the curves for the linear response versus signal frequency. © *2005 American Institute of Physics*. [DOI: 10.1063/1.1899287]

Noise plays an important role in the understanding and description of nature. In contrast to the usual role of noise as a nuisance, under certain conditions noise can also play a constructive ("ordering") role in nonlinear systems far from equilibrium. Properly stochastic resonance[1,2] (SR) is the most famous noise-induced effect and describes the enhancement of the system response to a signal due to optimal noise. We study a spatial extended excitable neuron-like system with an inhibitory coupling between oscillators. The excitable property provides a high nonlinear sensitivity to perturbations and to the signal near the rest state. The inhibitory coupling is required to induce stochastic multiresonance and can be found in many natural systems, e.g., in chemical systems with inhibitory diffusion[3] or in biological systems with competition.[4] Such a coupling provides coexistence of several average periods distinct from that of an isolated oscillator and several phase relations between the elements.[5,6] In the present work we exploit the multirhythmicity evoked by the inhibitory coupling to enhance information exchange along a noisy chain of oscillators in certain frequency bands. In this case, noise plays two roles: it stimulates firing because the signal is below the excitation threshold, and causes switches between different attractors with varying phase relations in the ensemble. The appearance of these distinct stochastic attractors can be controlled by varying the signal period, noise intensity, and the point of signal application. The frequency- and noise-selective signal acceptance and penetration along the chain can be viewed as a particular kind of SR. The understanding of frequency-dependent SR should be useful in the analysis of multifrequency mechanisms of information exchange in neural networks and various diffusively coupled activator–inhibitor oscillator arrays in other fields, e.g., in chemistry or biology.

I. INTRODUCTION

The dynamics of self-oscillatory and excitable systems near the generation threshold has been a focus of interest for a long time because it is the region where their controllability is greatest. A recent surge of interest in this domain was initiated by studies on coherence resonance[7,8] and stochastic resonance (SR) in nonlinear excitable units.[1,9–11] The parameter region near the Hopf bifurcation is also popular in models of isolated neurons[12,13] and was shown to be a likely source of multimodal oscillations in models of neuron ensembles.[14]

Spatiotemporal SR is the extension of the classical SR to networks and considers the noise-enhanced propagation of structures which could be found, e.g., in neural networks[15] or in the well-known photosensitive Belousov–Zhabotinsky.[16] Although there are several investigations of array-enhanced SR,[17,18] signal amplification in a spatial extended system as a function of the signal frequency has not yet been examined. In the studies cited, coupling was of a type that resulted in amplification of signals of any frequency. For isolated *excitable* systems, the dependence of SR on the signal period has only one maximum per period, and the latter nearly coincides with the excursion time of an excitable element. This time is the sole natural reference point for the time scale of the process.[19,20] Recently, it has been shown that frequency and phase locking in an ensemble of noise-stimulated excitable FitzHugh–Nagumo (FHN) oscillators can be enhanced by optimizing the number of the coupled elements;[21,22] however, the frequency dependence of signal enhancement was very similar to that for an isolated element. Analogous results have been obtained in the framework of the Hindmarsh–Rose neuronal model.[23]

In this study, we examine effects of the signal frequency on the signal processing in a linear chain of four excitable oscillators coupled via inhibitor diffusion (slow variable exchange). Models of oscillatory media with inhibitory coupling exhibit very rich dynamics and are commonly used to describe various physical,[24] electronic,[25] or chemical

[a)]Electronic mail: volkov@lpi.ru
[b)]Electronic mail: ullner@agnld.uni-potsdam.de
[c)]Electronic mail: jkurths@agnld.uni-potsdam.de

systems.[26,27] In chemistry, an effective increase in inhibitor diffusion, which is usually attained by reducing the activator diffusivity through a complexing iodide (activator) with starch macromolecules, leads to a Turing structure formation.[3] In biology, the inhibitory form of coupling is used to explain morphogenesis in Hydra regeneration and animal coat pattern formation.[28] Recently, experimental studies of artificial gene networks have been summarized in mathematical models describing oscillators synchronized via slow autoinducer diffusion.[29,30] Competition in biological system is a source of spatial nonuniformities and motivates inhibitory coupling.[4] The dominance of this kind of coupling between identical oscillators was shown to give rise to many limit cycles of different periods and with different phase relations[5,6] which are stable in large regions of the control parameter space. This kind of coupling is usually referred to as "dephasing"[31,32] or "phase-repulsive"[33] interaction, because large regions in the phase space exist where the phase points repel one another owing to this interaction. Dephasing was shown to be a source of multirhythmicity in different systems.[25,34–36]

With excitable noisy elements, a dephasing interaction of stochastic limit cycles (instead of deterministic ones) may result in the coexistence of spatiotemporal regimes selectively sensitive to external signal periods. In such systems, noise plays at least two roles: First, it stimulates firing of stable elements and, thereby, their interaction during return excursions. Second, it stimulates transitions between coupling-dependent attractors if the lifetime thereof is sufficiently long. Our previous work[37] was limited to two and three elements coupled by inhibitor diffusion, for which the attractor structure is relatively simple. In a chain of *four* oscillators, only two simple antiphase modes can be observed. In one mode, the two middle elements move in phase with each other and in antiphase with the edge ones. In the other mode, every two adjacent elements move in antiphase. Under the same set of parameters, a four-oscillator chain can also oscillate in a complex manner with different partial limit cycles and complex phase relations between the elements. In this regime, its eight-dimensional limit cycle is such that the edge elements make two turns, generating two spikes at different interspike intervals, while the middle elements make only one turn. When attractors which have such different periods and phase relations compete among one another, multiple resonances in signal processing are likely to occur.

The paper is structured as follows. After the explanation of the model equations and the method used to estimate the signal processing, we review the dynamics evoked by inhibitory coupling. Then, we study the signal acceptance of the linear chain of four inhibitor-coupled excitable oscillators. Thereby, we investigate the signal response of the coupled system to a global signal, a local signal at the first element, and a local signal at the second element for different signal periods. A very rich multiresonance behavior appears in a noisy environment which is based on different phase relations between the oscillators. Since the signals are below the threshold of excitation, the stochastic limit cycle oscillations are noise evoked. After that, we explain the different phase relations and the associated distinct resonance frequencies at an unforced deterministic chain of four self-oscillatory elements. Next, we discuss every resonance peak and link these peaks with the favored phase relation of the stochastic attractor.

II. MODEL

We study an array of diffusively coupled stationary but highly excitable FitzHugh–Nagumo models (FHN) in the presence of white additive noise and forcing with subthreshold periodic signals applied to selected elements. The FHN model is a paradigmatic model describing the firing behavior of neurons[38] and, more generally, the activator–inhibitor dynamics of excitable media.[39]

The model is given by the following equations:

$$\frac{dx_1}{dt} = a - y_1 + \xi_1 + A_{s1}\cos\left(\frac{2\pi}{T_s}t\right) + C(x_2 - x_1), \tag{1}$$

$$\frac{dx_2}{dt} = a - y_2 + \xi_2 + A_{s2}\cos\left(\frac{2\pi}{T_s}t\right) + C(x_1 - x_2) + C(x_3 - x_2), \tag{2}$$

$$\frac{dx_3}{dt} = a - y_3 + \xi_3 + A_{s3}\cos\left(\frac{2\pi}{T_s}t\right) + C(x_2 - x_3) + C(x_4 - x_3), \tag{3}$$

$$\frac{dx_4}{dt} = a - y_4 + \xi_4 + A_{s4}\cos\left(\frac{2\pi}{T_s}t\right) + C(x_3 - x_4), \tag{4}$$

$$\varepsilon\frac{dy_i}{dt} = x_i - \frac{y_i^3}{3} + y_i, \tag{5}$$

where, in a neural context, $y_i(t)$ represents the membrane potential of the neuron and $x_i(t)$ is related to the time-dependent conductance of the potassium channels in the membrane.[38] The dynamics of the activator variable y_i is much faster than that of the inhibitor x_i, as indicated by the small time-scale-ratio parameter ε. It is well known that for $|a|>1$ the only attractor is a stable fixed point. For $|a|<1$, the limit cycle generates a periodic sequence of spikes. We fix a close to the bifurcation in the interval [1.01, 1.03] in order not to use high-level noise to excite oscillations and thereby to avoid masking of the fine structure of the interspike interval histograms. Here, ε is in the range [0.0001, 0.001], which is significantly smaller compared to those that are commonly used. This stiff excitation is needed to ensure a fast jumping between the attractors. The stochastic forcing is represented by a Gaussian white noise $\xi_i(t)$ with zero mean and intensity σ_a^2: $\langle \xi_i(t)\xi_j(t+\tau)\rangle = \sigma_a^2\delta(\tau)\delta_{i,j}$. The harmonic signal is subthreshold, $A_{si} < a - 1.0$ and is added to the slow variables inputs. Previous investigations of isolated FHN (Ref. 1) show that SR properties do not depend on which variables signal and noise are applied. To evaluate the amplitude of the input frequency in the output signal, we calculate the linear response Q at the input frequency $\omega = 2\pi/T_s$:[2,40]

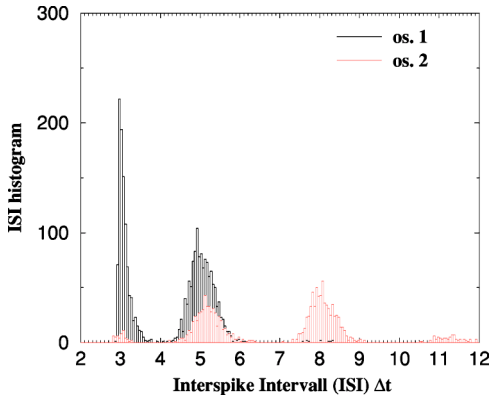

FIG. 1. ISI distributions for the oscillators (os.) 1 and 2 of Eqs. (1)–(5) for $a=1.01$, $C=0.1$, $\varepsilon=0.0001$, no signal (i.e., $A_{si}=0.0$) and $\sigma_a^2=5\times10^{-6}$. The histograms observed for elements 3 and 4 are similar. All histograms are based on time series of a fixed length of 9600 time units.

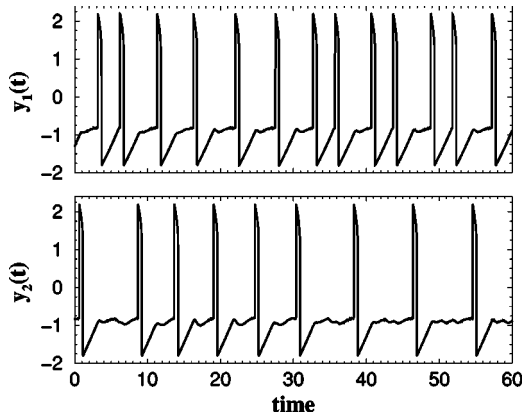

FIG. 2. Manifestation of the two stochastic regimes in the time series of the activator (fast) variable of oscillators 1 and 2 to illustrate the dynamics behind Fig. 1. The parameter are the same as in this figure for the ISI distribution: $a=1.01$, $C=0.1$, $\varepsilon=0.0001$, no signal (i.e., $A_{si}=0.0$), and $\sigma_a^2=5\times10^{-6}$.

$$Q_{\sin}=\frac{\omega}{2n\pi}\int_0^{2\pi n/\omega}2y(t)\sin(\omega t)dt, \tag{6}$$

$$Q_{\cos}=\frac{\omega}{2n\pi}\int_0^{2\pi n/\omega}2y(t)\cos(\omega t)dt, \tag{7}$$

$$Q=\sqrt{Q_{\sin}^2+Q_{\cos}^2}, \tag{8}$$

when n is the number of periods T_s, covered by the integration time. Equations (6) and (7) represent the Fourier coefficients of the signal frequency in the output.

The equations were solved numerically using a fourth-order double-precision Runge–Kutta routine, the Heun algorithm,[41] and the Helfand algorithm.[42] To ensure that the results were not a numerical artifact or long-lived transients, we tested whether they varied depending on the method used and the accuracy set in computations. The algorithms for seeking and identifying the attractors were based on randomly varying the initial points and observing the dynamics of interspike intervals of each oscillator during the settling of the systems on the attractor. After an attractor was detected, its boundaries were determined by slowly varying one or two parameters and correcting the step size for given parameter values in case stability was lost.

III. REVIEW OF THE DYNAMICS EVOKED BY INHIBITORY COUPLING

In order to get a reference frame for further comparisons, we begin with noise-induced interspike interval (ISI) distributions for our excitable system ($a=1.01$) in the absence of external forcing. Figure 1 shows the ISI histograms for the first two elements calculated for a noise level $\sigma_a^2=5\times10^{-6}$ and a small coupling strength. This noise level was found to be optimal in demonstrating multimode behavior of coupled identical excitable elements. The multimode behavior is caused by the different stochastic attractors with different typical spike distances and the stochastic switching between them. In contrast to that, the multimode behavior in the ISI histograms of a single bistable system subjected to a subthreshold signal and weak noise[43] is equal spaced and caused by integer multiple of the signal period, and so the mechanism of multimode behavior in the ISI histogram is different from our setup. Noise amplitude variation results in changes in the extent of coherence in the system's behavior, because the attractors with different time scales are induced by different noise intensities. The possibility of manipulating the extent of coherence in this way has already been demonstrated experimentally[44] and numerically[45] for systems of two and three coupled excitable elements.

In Fig. 1, one can clearly see several time scales different from the excursion time of an isolated element ($T_{\text{exc}}\approx2.8$). Despite the fact that the elements are identical, the distances between the peaks in the histogram are different. The interspike intervals from oscillators 1 and 2 are the major contributors to the first and third peaks, respectively, whereas the second peak contains the intervals produced by both elements but with different frequency. This structure of the ISI histograms suggests that the system has more than one noise-induced stochastic limit cycle. The stochastic switching between two dominant regimes can be seen in the time series of Fig. 2 also. The first oscillator exhibits prefer-

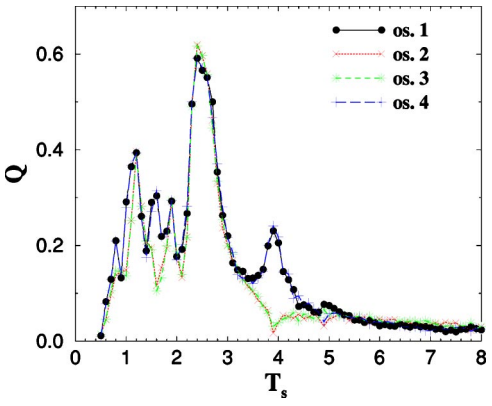

FIG. 3. The dependence of the linear response Q [Eq. (8)] for the 4 FHNs on the signal period T_s for the noise level 1×10^{-5} by global subthreshold signal ($A_{s1,2,3,4}=0.01$). The other parameters are $\varepsilon=0.0001$, $a=1.01$, and $C=0.1$.

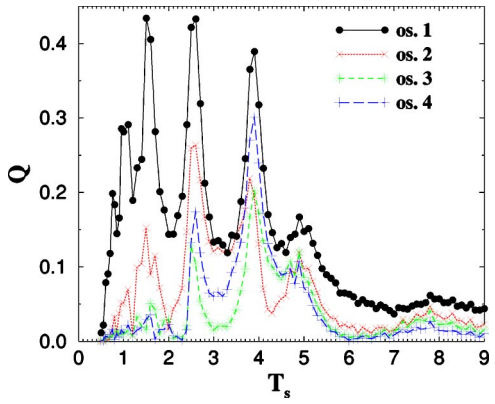

FIG. 4. The dependence of the linear response Q [Eq. (8)] for the 4 FHNs on the signal period T_s for the noise level 1×10^{-5}. The signal is applied to the first element only ($A_{s1}=0.01$ and $A_{s2,3,4}=0.0$). The other parameters are $\varepsilon=0.0001$, $a=1.01$, and $C=0.1$.

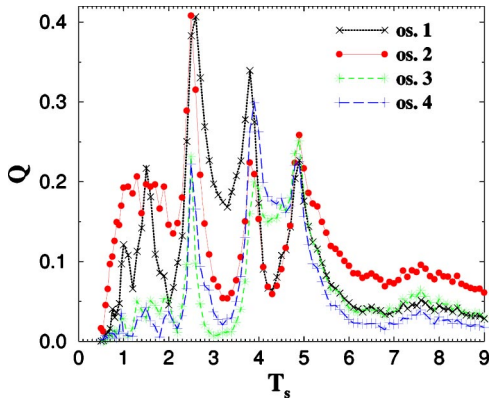

FIG. 5. The dependence of the linear response Q [Eq. (8)] for the 4 FHNs on the signal period T_s for the noise level 1×10^{-5}. The signal is applied to the second element only ($A_{s2}=0.01$ and $A_{s1,3,4}=0.0$). The other parameters are $\varepsilon=0.0001$, $a=1.01$, and $C=0.1$.

entially spike distances of about 3.0 and 4.8, whereas spike distances of about 5.1 and 8.0 dominate in the dynamics of the second oscillator. The time series demonstrate the phase relations between the spikes in different oscillators also, and make clear the inhibitory nature of the coupling via the slow inhibitor variable.

IV. SIGNAL ACCEPTANCE BY EXCITABLE SYSTEMS

Next, we add an external periodic signal capable of interacting with the stochastic attractors and analyze the dynamics for different noise levels. Our goal is to select the most representative results that hold in large intervals of noise intensities. Figure 3 shows the presence of a global subthreshold signal in the output of each element. Multiple resonances in the signal acceptance are clearly seen.

One can clearly see in Fig. 3, at $T\approx1.5$ and $T\approx3.9$ (regions of resonance), the Q curves for the middle and edge elements behave oppositely (i.e., the Q maximum for the edge elements corresponds to the Q minimum for the middle ones), suggesting that a signal applied simultaneously to all elements (global signal) can selectively suppress its own manifestation in the middle elements, while stimulating an acceptance in the edge elements.

When a signal is applied to the first element 1 (Fig. 4), multiple resonances are even more pronounced than in Fig. 3 and the curves for all elements become similar in shape. However, $Q_4>Q_{2,3}$ around $T_s=3.9$, i.e., if the signal period is $T_s\approx3.9$, the signal travels throughout the chain despite low values of $Q_{2,3}$. The multipeak structure of $Q(T_s)$ is conserved if the entry of the signal is the second element (Fig. 5). However, the peak amplitudes are changed. Let us highlight again the resonance peak at $T_s\approx3.9$: The response of the first and last oscillator is much higher than the response of the middle one ($Q_{1,4}>Q_{2,3}$), despite the fact that the second element (filled circuits in Fig. 5) is the driven element and is the one most affected by the signal. This unexpected order illustrates the high reliability of the underlying phase regime, which we refer to and explain in the next section as the intricate R(2,1,1,2) attractor.

This frequency selectivity is reflected in the appearance of additional peaks (Fig. 6) in the standard characteristic of SR (system response Q versus noise intensity). In contrast to isolated excitable elements or fast-variable-coupled arrays, a chain of four elements coupled via a slow variable exchange exhibits additional SR peaks, whose positions and amplitudes depend on the periods of the applied signals. This observation pertains to the ″stochastic multiresonance″ phenomenon (see, e.g., Ref. 46 and reference therein), extended to encompass its dependence on the external signal period.

The effects described above depend not only on the very large stiffness, but also on the other model parameters: the coupling strength and the proximity of the bifurcation pa-

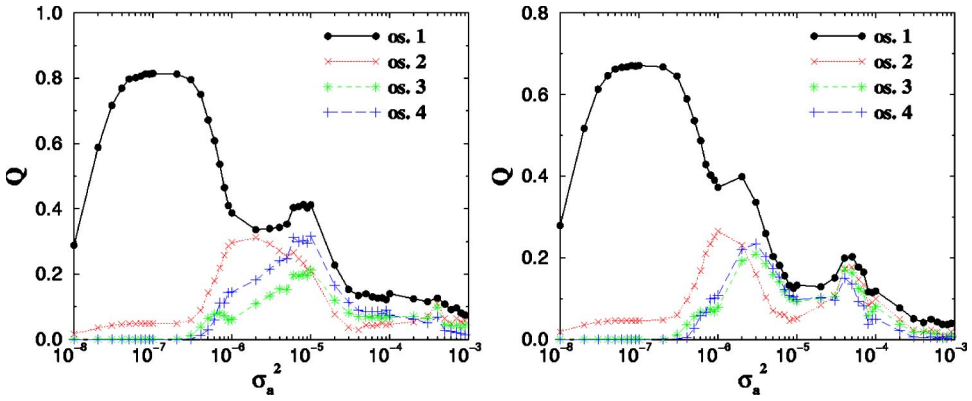

FIG. 6. The dependencies of the linear response Q for a chain of four elements [Eqs. (1)–(5)] as a function of the noise intensity for different signal periods: $T_s=3.9$ (left) and 4.5 (right). The signal of the amplitude $A_{s1}=0.01$ is applied to the first oscillator only ($A_{s2,3,4}=0.0$). The other parameters are $a=1.01$, $\varepsilon=0.0001$, and $C=0.1$.

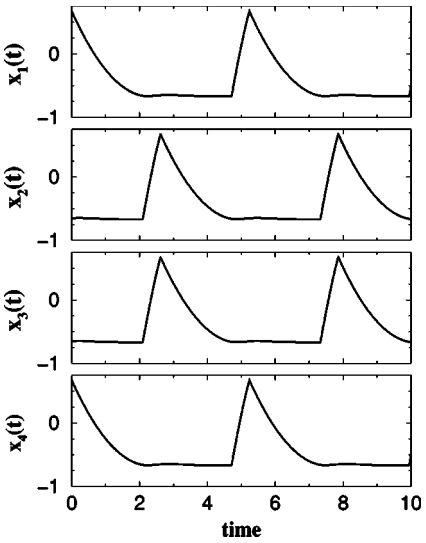

FIG. 7. Waveforms of the slow variables for the antiphase attractor A1 calculated for $a=0.99$ and $C=0.2$. Moving along a segment of the trajectory near $x_i=-0.66$, the representative point slowly approaches the firing point. After the spike, an abrupt increase in the slow variable is observed. No signal ($A_{s1,2,3,4}=0.0$) and no noise ($\sigma_a^2=0.0$) are added to demonstrate the pure unperturbed mode A1.

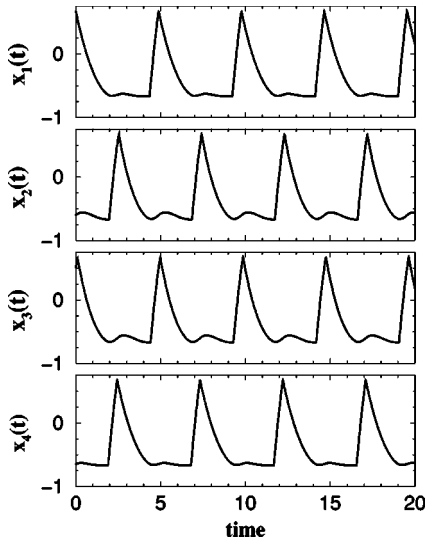

FIG. 8. Waveforms of the slow variables for the antiphase attractor A2 calculated for $C=0.2$ and $a=0.99$. No signal ($A_{s1,2,3,4}=0.0$) and no noise ($\sigma_a^2=0.0$) are added to demonstrate the pure unperturbed mode A2.

rameter a to the bifurcation value. Our analysis showed that the results remain valid over an at least twofold range of coupling strengths and over a twofold range of values of the difference $(a-1.0)$.

In order to clarify how multiple resonances arise, we shall draw on the similarity between stochastic and deterministic limit cycles. The proximity of the bifurcation parameter to the Andronov–Hopf bifurcation and the large stiffness of oscillators allow us to compare our excitable chain to its deterministic self-oscillatory version.

V. COUPLED DETERMINISTIC OSCILLATORS

Discussing the possible dynamic modes, we have to consider first the in-phase attractor, which is formally stable with this type of coupling but has a small basin of attraction. Our numerical analysis shows that the system leaves this attractor if the slow variable of one of the oscillators is more than $(2\%-3\%)$ smaller than those of the other ones. For a chain of four units, two antiphase modes are possible. In one mode referred to as A1 below, strictly antiphase waveforms are observed: unit 2 moves in phase with unit 3 and in antiphase with units 1 and 4 (Fig. 7). In mode A2, the phase shift between units 1 and 3 is almost vanishing, whereas units 2 and 4 oscillate almost in antiphase relative to units 1 and 3, respectively (Fig. 8). Obviously, mode A1 coincides with the antiphase mode in a system of two units because, due to the synchronous run of the units 2 and 3 in this regime, the diffusion between these elements goes effectively to zero and does not affect these neighbors. Hence, units 2 and 3 are not coupled by a slow variable exchange. Similar to the pure in-phase motion, the basin of attraction of this mode A1 is not large: even if the representative points of units 2 and 3 diverge only slightly, the systems are brought out of mode A1.

Mode A2 is one of the basic attractors in the configuration under consideration (Fig. 8). Variation in the number of neighbors (oscillators 1 and 4 each have one neighbor, whereas oscillators 2 and 3 each have two neighbors) results in a behavior not exactly antiphase. An analysis of how the waveform changes as the parameter a approaches the bifurcation point shows that, the closer the approach, the more clearly the oscillations observed are of the antiphase type. In addition, variation in the number of neighbors leads to the trajectories of units 1 and 4 near the firing point behaving differently compared with the trajectories of units 2 and 3.

It is essential to include this variation in the analysis of the effects due to the external signals and noise on such a chain, because it is this part of the trajectory that is most sensitive to external forcing. In this study, we examine only the range of a values from 0.95 close to 1.0, which is of crucial importance for understanding the dynamics of excitable systems with inhibitory coupling. Mode A2 can be detected at low coupling strengths, say, at $C=0.02$. However, the in-phase and antiphase modes have very close periods in this region of small coupling strength. Despite the differences in phase relations, the periods of attractors A1 and A2 are very close to each other in a broad range of coupling strengths ($T_{\text{anti}}=5.2$ if $C=0.1$).

If the coupling strength is not very low, an intricate limit cycle can arise in a linear chain that we designate as R(2,1,1,2). This designation indicates that the cycle period is equal to one interspike interval for units 2 and 3 but contains two interspike intervals for units 1 and 4 (Fig. 9); ($T_1=T_4=2.8+4.7, T_2=T_3=7.5$).

The basis for the formation of this attractor is a kind of "internal" synchronization of individual oscillators. Their periods become prolonged in the presence of inhibitory coupling, because it takes them longer to reach the firing point. The number of spikes that individual units generate depends on their phase relations. The inner units experience three delays, which are clearly seen in the waveforms of unit 2 and

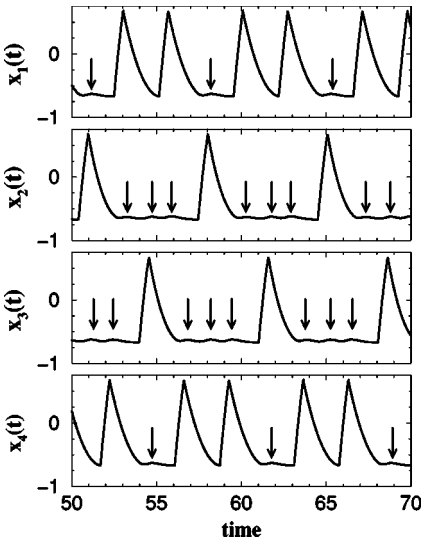

FIG. 9. Waveforms of the slow variables for the intricate R(2,1,1,2) attractor, as calculated for $a=0.98$ and $C=0.2$. No signal ($A_{s1,2,3,4}=0.0$) and no noise ($\sigma_a^2=0.0$) are added to demonstrate the pure unperturbed mode R(2,1,1,2). The arrows highlight the corresponding subthreshold response to spikes of the neighbor oscillators due to the inhibitory coupling.

3 shown in Fig. 9 by three local subthreshold maxima between large spikes (highlighted by the three arrows between two consecutive spikes). The firing of element 2 is delayed first by interaction with unit 1. Their interaction draws the representative point away from the firing point. The second delay is due to its interaction with unit 3, and the third delay is again because of an interaction with unit 1. For the outer oscillators, only one delay is possible. Their periods are determined mainly by the parameter a, i.e., by the time required for an isolated oscillator to pass though the cycle. In the two-dimensional phase plane of each oscillator, this mode for unit 1 and 4 looks like a doubled limit cycle, along which the phase points make two turns per period, while the inner oscillators make just one turn. The farther parameter a is from the bifurcation, the shorter is the main cycle, and the shorter are the delays. In this way, other phase relations arise, forming the mode R(4,3,3,4) and other similar modes, which are beyond the scope of this study, because we are interested only in modes near the oscillation threshold of isolated oscillators.

VI. DISCUSSION

We suggest that it is the complex structure of the intricate attractor R(2,1,1,2) (Fig. 9) that provides for the existence of the large peaks at $T_s\approx 1.5$, $T_s\approx 3.9$, while the antiphase regime is responsible for the peaks at $T_s\approx 1.25$, $T_s\approx 2.5$, and $T_s\approx 5$. Obviously, the latter arise as a result of 1:4, 1:2, and 1:1 synchronization with stochastic antiphase oscillations. The average period of this stochastic regime ($\langle T\rangle=4.8$; see Figs. 1 and 2) is slightly shorter than that of the deterministic one ($T=5.2$) because noise induces the premature jumping of representative points to the other branch of the N-shaped null cline and thereby reduces the attractor period.

In order to demonstrate the influence of interesting signal periods on the probability of emergence and existence of a particular attractor during a long noise-induced process, the ISI histograms were calculated for the signal periods $T_s=3.1$ (small Q) and $T_s=3.9$ (large Q) (see Fig. 10 and compare with Fig. 1).

As can be seen in Fig. 10 (left), for a signal period $T_s=3.1$, the histogram peaks are slightly lower and broader than in the absence of external forcing. In contrast, a signal of period $T_s=3.9$ [Fig. 10(right)] increases significantly the relative height of the peak at $T\approx 7.6$. This peak contains the ISIs emerging from the regime R(2,1,1,2). Interestingly, the ISI values of about 3.9 are absent in the histograms, although such signals support the stochastic version of R(2,1,1,2) and their acceptance is good (the largest value of Q). In other words, in the presence of a signal of period $T_s=3.9$, the regime R(2,1,1,2) is more likely to be observed than the antiphase one. The last statement concerning $T_s=3.9$ is less obvious compared with the statement that the signal of period $T_s=2.4$ (which is half the T_{anti}) is compatible with the antiphase regime. Therefore, we present segments of stochastic time series for units 1 and 2 and the signal waveform that demonstrate microscopically how the signal increases the probability of the R(2,1,1,2) regime (Fig. 11).

At the signal minima, the parameter a is brought closer to the bifurcation point $a=1$ (signal is negative). At the signal maxima, a is pulled away from the bifurcation point, making firing less probable. It is easy to see that firings frequently occur when the signal is negative, and that the two

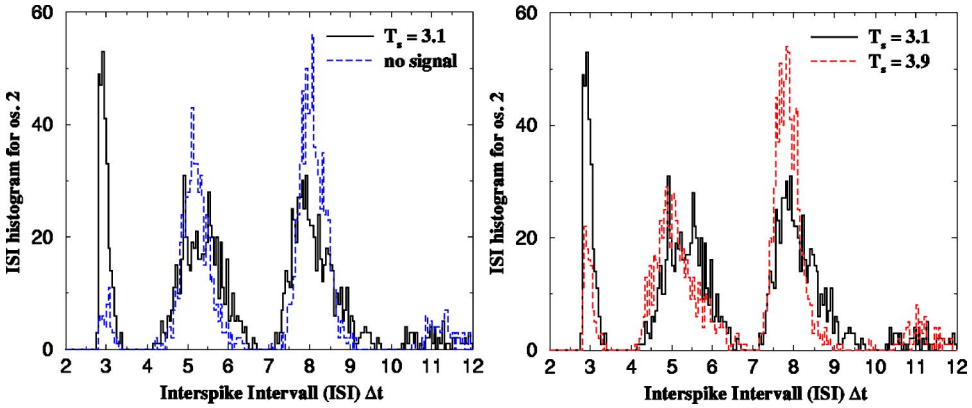

FIG. 10. The ISI distributions for element 2 for $a=1.01$, $C=0.1$, $\sigma_a^2=5\times10^{-6}$, $\varepsilon=0.0001$, $T_s=3.1$ (solid line in both diagrams) and $T_s=3.9$ (dashed line, right), respectively. The signal is applied to unit 1 with $A_{s1}=0.01$. For comparison, the dashed line in the left diagram denotes the unforced situation ($A_{s1,2,3,4}=0.0$) as in Fig. 1. All histograms are based on time series with a fixed length of 9600 time units.

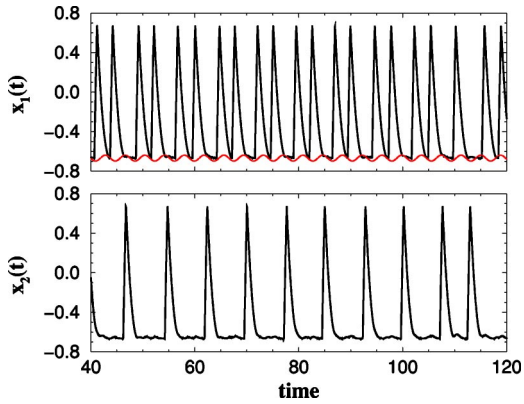

FIG. 11. Stochastic waveforms of the slow variables for $\varepsilon=0.0001$, $a=1.01$, $C=0.1$, $\sigma_a^2=10^{-5}$, $T_s=3.9$, and $A_{s1}=0.01$ (signal applied to the first oscillator only). The periodic curve illustrates the periodic signal (which acts on the first element only) with a three times increased amplitude than in the calculations for a better recognition of the synchronization between input and output. The periodic input signal is shifted to the fixed point.

periods of this signal are usually equal to the sum of two consecutive ISIs.

The same explanation of resonance is valid for a signal of period $T_s=1.5$ applied to unit 1 (Fig. 4). The most probable ISIs observed for unit 1 are around 4.5 and 3.0, which are $3T_s$ and $2T_s$, respectively. However, forcing with a high-frequency signal results in the fuzzy control of the ISIs along the chain. This means that the signal is consistent with the set of the phase relations of R(2,1,1,2) but fluctuations of ISIs values grow with the unit number and hence decrease the signal penetration along the chain. Therefore, $Q_1 \gg Q_4$ for $T_s=1.5$.

VII. CONCLUSION

In summary, we have demonstrated that both signal propagation and acceptance are frequency selective in a noisy system of excitable inhibitory coupled units, to which a subthreshold harmonic signal is applied. In such systems, the constructive role of noise depends strongly on the signal period. The multiresonances detected by calculating the linear response Q versus the signal period T_s for global and local signals at appropriate noise levels are even more pronounced than SR that are detected in a standard way by calculating the well-known function Q versus noise intensity σ_a^2 for a fixed signal period.

The mechanism behind this selectivity is that new resonance frequencies (other than the resonance frequency of an isolated FHN) arise in a system of coupled oscillators because of the phase shifts between them. Shifting the control parameter a from the excitable to the oscillatory regime, we have found a set of stable deterministic attractors and suggested that a very small shift in the parameter a and a very large stiffness ensure the similarity between the deterministic and the stochastic isolated limit cycles. In the presence of coupling, the deterministic set of attractors may be richer than the stochastic set because noise can mask attractors with small basins. In a noisy environment, the antiphase regime and the complex R(2,1,1,2) regime are more or less long-lived attractors, which exist one at a time. When one of both disappears, the other sets in. Forcing an element of the network in resonance with one of these coupling-dependent resonance frequencies, we obtain not only the typical bell-shaped curve of standard SR, but remarkable additional resonance peaks too.

The study of frequency-dependent SR will be useful in gaining a better understanding of multifrequency mechanisms of information exchange in neural networks. Because of the generality of these effects across various diffusively coupled activator–inhibitor oscillator arrays, including FHN systems, we expect that these findings can also be applicable in other fields, e.g., in chemistry or biology.

ACKNOWLEDGMENTS

E.V., E.U., and J.K. acknowledge financial support from SFB 555 (Germany) and Program "Radiofizika" of Russian Academy (E.V.). E.V. acknowledges the Russian Foundation for Basic Research (02-01-00064) and a grant from the President of the Russian Federation for financial support.

[1] B. Lindner, J. García-Ojalvo, A. Neiman, and L. Schimansky-Geier, Phys. Rep. **392**, 321 (2004).
[2] L. Gammaitoni, P. Hänggi, P. Jung, and F. Marchesoni, Rev. Mod. Phys. **70**, 223 (1998).
[3] I. Lengyel and I. Epstein, Science **251**, 650 (1991).
[4] G. Balázsi, A. H. Cornell-Bell, and F. Moss, Chaos **13**, 515 (2003).
[5] E. I. Volkov and M. N. Stolyarov, Phys. Lett. A **159**, 61 (1991).
[6] E. I. Volkov and M. N. Stolyarov, Biol. Cybern. **71**, 451 (1994).
[7] H. Gang, H. Haken, and X. Fagen, Phys. Rev. Lett. **77**, 1925 (1996).
[8] A. Pikovsky and J. Kurths, Phys. Rev. Lett. **78**, 775 (1997).
[9] F. Moss, J. Douglass, L. Wilkens, D. Pierson, and E. Pantazelou, Ann. N.Y. Acad. Sci. **706**, 26 (1993).
[10] K. Wiesenfeld, D. Pierson, E. Pantazelou, C. Dames, and F. Moss, Phys. Rev. Lett. **72**, 2125 (1994).
[11] V. S. Anishchenko, A. B. Neiman, F. Moss, and L. Schimansky-Geier, Phys. Usp. **42**, 7 (1999).
[12] V. A. Makarov, V. I. Nekorkin, and M. G. Velarde, Phys. Rev. Lett. **86**, 3431 (2001).
[13] E. M. Izhikevich, BioSystems **67**, 95 (2002).
[14] G. Medvedev, C. Wilson, J. Callaway, and N. Kopell, J. Comput. Neurosci. **15**, 53 (2003).
[15] G. Balázsi, L. B. Kish, and F. E. Moss, Chaos **11**, 563 (2001).
[16] S. Kádár, J. Wang, and K. Showalter, Nature (London) **391**, 770 (1998).
[17] J. Lindner, B. Meadows, W. Ditto, M. Inchiosa, and A. Bulsara, Phys. Rev. Lett. **75**, 3 (1995).
[18] J. Lindner, J. Mason, J. Neff, B. Breen, W. Ditto, and A. Bulsara, Phys. Rev. E **63**, 041107 (2001).
[19] S. R. Massanés and C. J. P. Vicente, Phys. Rev. E **59**, 4490 (1999).
[20] T. Kanamaru, T. Horita, and Y. Okabe, Phys. Lett. A **255**, 23 (1999).
[21] C. Zhou, J. Kurths, and B. Hu, Phys. Rev. Lett. **87**, 098101 (2001).
[22] R. Toral, C. Mirasso, and J. D. Gunton, Europhys. Lett. **61**, 162 (2003).
[23] F. Liu, J. Wang, and W. Wang, Phys. Rev. E **59**, 3453 (1999).
[24] B. Kerner and V. Osipov, Sov. Phys. Usp. **33**, 679 (1990).
[25] D. Ruwisch, M. Bode, D. Volkov, and E. Volkov, Int. J. Bifurcation Chaos Appl. Sci. Eng. **9**, 1969 (1999).
[26] V. Vanag, L. Yang, M. Dolnik, A. Zhabotinky, and I. Epstein, Nature (London) **406**, 389 (2000).
[27] V. Castets, E. Dulos, J. Boissonade, and P. D. Kepper, Phys. Rev. Lett. **64**, 2953 (1990).
[28] H. Meinhardt, *Models of Biological Pattern Formation* (Academic Press, New York, 1982).
[29] D. McMillen, N. Kopell, J. Hasty, and J. J. Collins, Proc. Natl. Acad. Sci. U.S.A. **99**, 679 (2002).
[30] A. Kuznetsov, M. Kærn, and N. Kopell, SIAM J. Appl. Math. **65**, 392 (2004).
[31] S. K. Han, C. Kurrer, and Y. Kuramoto, Phys. Rev. Lett. **75**, 3190 (1995).
[32] D. Postnov, S. K. Han, and H. Kook, Phys. Rev. E **60**, 2799 (1999).
[33] G. Balázsi, A. Cornell-Bell, A. B. Neiman, and F. Moss, Phys. Rev. E **64**, 041912 (2001).

[34]A. Sherman and J. Rinzel, Proc. Natl. Acad. Sci. U.S.A. **89**, 2471 (1992).
[35]G. S. Cymbalyuk, E. V. Nikolaev, and R. M. Borisyuk, Biol. Cybern. **71**, 153 (1994).
[36]E. I. Volkov and D. V. Volkov, Phys. Rev. E **65**, 046232 (2002).
[37]E. Volkov, E. Ullner, A. Zaikin, and J. Kurths, Phys. Rev. E **68**, 061112 (2003).
[38]J. P. Keener and J. Sneyd, *Mathematical Physiology* (Springer, New York, 1998).
[39]A. S. Mikhailov, *Foundations of Synergetics*, 2nd ed. (Springer, Berlin, 1994),
[40]P. Landa and P. McClintock, J. Phys. A **33**, L433 (2000).
[41]J. García-Ojalvo and J. M. Sancho, *Noise in Spatially Extended Systems* (Springer, New York, 1999).
[42]E. Helfand, Bell Syst. Tech. J. **58**, 2289 (1979).
[43]A. Longtin, A. Bulsara, and F. Moss, Phys. Rev. Lett. **67**, 656 (1991).
[44]D. E. Postnov, O. V. Sosnovtseva, S. K. Han, and W. S. Kim, Phys. Rev. E **66**, 16203 (2002).
[45]E. Volkov, M. Stolyarov, A. Zaikin, and J. Kurths, Phys. Rev. E **67**, 066202 (2003).
[46]S. Matyjaśkiewicz, A. Krawiecki, J. Hołyst, and L. Schimansky-Geier, Phys. Rev. E **68**, 016216 (2003).